

Optimization of Transition Manoeuvres for a Tail-Sitter Unmanned Air Vehicle (UAV)

R.H. Stone^{*}, G. Clarke[†],

Abstract

This paper describes work done in optimizing the transition manoeuvres between vertical and horizontal flight for a tail-sitter unmanned air vehicle. This work is part of an ongoing research program involving the construction and test of a concept demonstrator tail-sitter UAV, the “T-Wing,” that is being undertaken by the University of Sydney in collaboration with Sonacom Pty Ltd. The use of an unmanned air-vehicle (UAV) with a vertical take-off and landing (VTOL) capability that can still enjoy efficient horizontal flight promises significant operational advantages over other vehicles. However, the transition between these phases of flight is one problem that needs to be addressed to make the vehicle effective. This paper looks at using numerical optimization techniques coupled with a 6-DOF non-linear model of the vehicle to obtain the best possible transition maneuvers in terms of minimizing such things as the time to complete the transition and any excess height gain during the maneuver as well as avoiding unpredictable regions of the flight envelope.

Introduction

Rationale for a Tail-Sitter UAV

Because tail-sitter vehicles do not require runways, catapults, rocket assistance, nets, parachutes or airbags for take-off and landing they promise greater operational flexibility in many environments than conventional UAVs. As well, by utilising a winged horizontal flight mode they also promise considerable performance gains in comparison to helicopter like vehicles. A further benefit that a tail-sitter vehicle possesses in comparison to other competing vehicles such as tilt-rotors, tilt-wings and tilt-bodies is mechanical simplicity and hence lower weight. This benefit is enhanced even further by doing away with conventional helicopter rotor heads and replacing them with simpler variable pitch propellers. In this scheme the vehicle is controlled in the hover via prop-wash over wing and fin mounted control surfaces.



Figure 1: A Typical UAV Mission: Deployment and Monitoring of Acoustic Sensors

^{*} Department of Aeronautical Engineering, University of Sydney

[†] Sonacom Pty Ltd

An obvious example of the use of a tail-sitter UAV would be as a surveillance platform launched from the back of a frigate as shown in Figure 1. In this role the UAV might be called upon to deploy and monitor sonobuoys as well as provide other reconnaissance information. Due to the numerous perceived advantages of tail-sitter vehicles, the University of Sydney and Sonacom Pty Ltd have embarked on a collaborative research programme (via a SPIRT grant) to build and test a concept demonstrator vehicle. It is hoped that this will pave the way for the use of these types of vehicles in both military and civilian markets.

The Current Vehicle

The proposed *T-Wing* vehicle is somewhat similar to the Boeing Heliwing of the early 1990s in that it also has twin wing-mounted propellers, however it differs from that vehicle in a number of important respects.

- In keeping with the basic simplicity of the tail-sitter configuration, control is effected via prop-wash over the wing and fin mounted control surfaces, rather than using helicopter cyclic control. This is similar to the early tail-sitter vehicles of the 1950s, the Convair XF-Y1 and the Lockheed XF-V1. Collective blade pitch control is still required to achieve efficient horizontal flight performance and produce adequate thrust on take-off.
- The current vehicle uses a canard to allow a more advantageous placement of the vehicle centre of gravity (CG).
- Two separate engines are used in the current design though the possibility of using a single engine with appropriate drive trains could also be accommodated.

A diagram of a typical vehicle showing some of the important gross geometric properties is given in Figure 2.

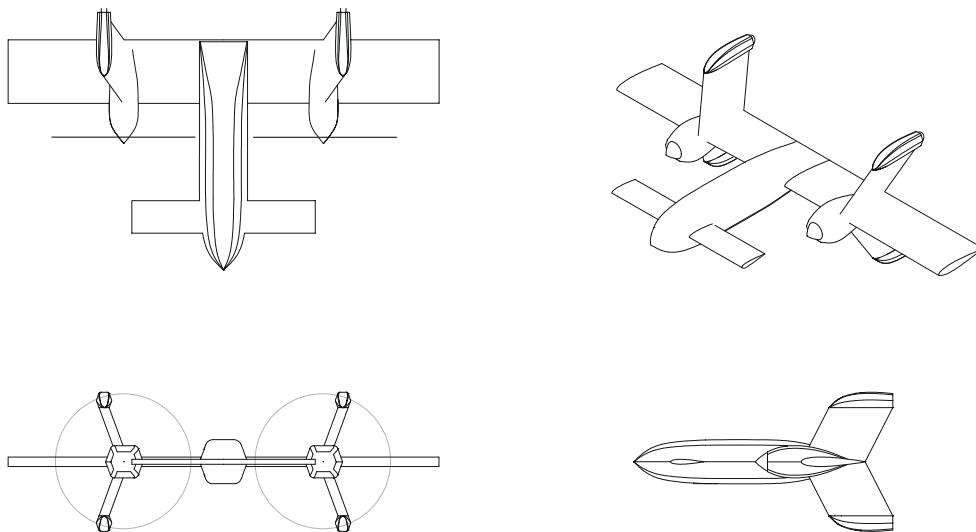


Figure 2: T-Wing Vehicle Configuration

Although a tentative maximum take-off weight (MTOW) of approximately 300-kg (660-lb) is envisaged for the full size *Mirli* vehicle, the concept demonstrator vehicle is considerably smaller, with an MTOW of approximately 50 lb. The demonstrator vehicle has a 7 ft (2.13 m) wingspan and a total length (from nose to fin tip) of 5 ft (1.52 m). The vehicle was originally designed to be powered by two, geared, 4.5 HP electric brushless DC motors driving 30 inch fixed pitch counter-rotating propellers and supplied by up to 20 lb (9.1 kg) of Ni-Cd batteries. This was designed to give the vehicle a maximum endurance of 5 - 6 minutes, which was long enough to accomplish the critical flight control objectives of demonstrating stable autonomous hover along with the two transition manoeuvres. The reason for initially selecting electric rather than petrol propulsion was because electric motors

promised easier set-up and operation in comparison to petrol engines. Unfortunately problems with the particular electric motor speed controllers selected caused excessive delays and doubts about system reliability. For these reasons, it was decided in August 2000 to convert the vehicle to run on petrol engines.

The petrol engine version uses two 6 HP 2-stroke motors and has the same nominal weight as the electric vehicle. The petrol engines drive two counter-rotating 23-inch fixed pitch propellers directly. For the sake of system simplicity there is no cross shafting between the two engines. Due to the higher installed power of the petrol engines this vehicle has considerably more excess thrust than the electric vehicle and it is anticipated that the MTOW can be pushed to at least 65-lb, (29.5-kg). Although the petrol vehicle is still very much a concept demonstration platform, this increased take-off weight should allow an endurance of up to several hours carrying a 5-lb payload.

The vehicle is built primarily of carbon-fibre and glass-fibre composite materials with local panel stiffness provided by the use of Nomex honeycomb core material. The airframe has been statically tested to a normal load factor in excess of 8 G's¹. A picture of the completed T-Wing vehicle is shown in Figure 3, while a picture of the vehicle undergoing initial flight trials in December 2000 is shown in Figure 4.



Figure 3: Completed T-Wing Technology Demonstrator Vehicle, (Electric Powered Configuration).



Figure 4: First Free Flight of T-Wing Technology Demonstrator Vehicle under Manual Control. (Note "training" undercarriage").

Typical Flight Path for the "T-Wing" Vehicle

From the beginning of the *T-Wing* concept in mid 1995 it was proposed that the vehicle be allowed to transition from vertical to horizontal flight via a stall-tumble manoeuvre. This was seen as offering the potential advantage of allowing the vehicle to "carry" less excess hover thrust capability than would be required if a smooth unstalled transition was mandated. The reverse transition manoeuvre is less novel and simply involves the vehicle performing a pull-up to regain a vertical attitude followed by a slow descent. The mission phase of flight is performed in the more efficient horizontal "aeroplane" mode of flight. This flight regime is shown in Figure 5.

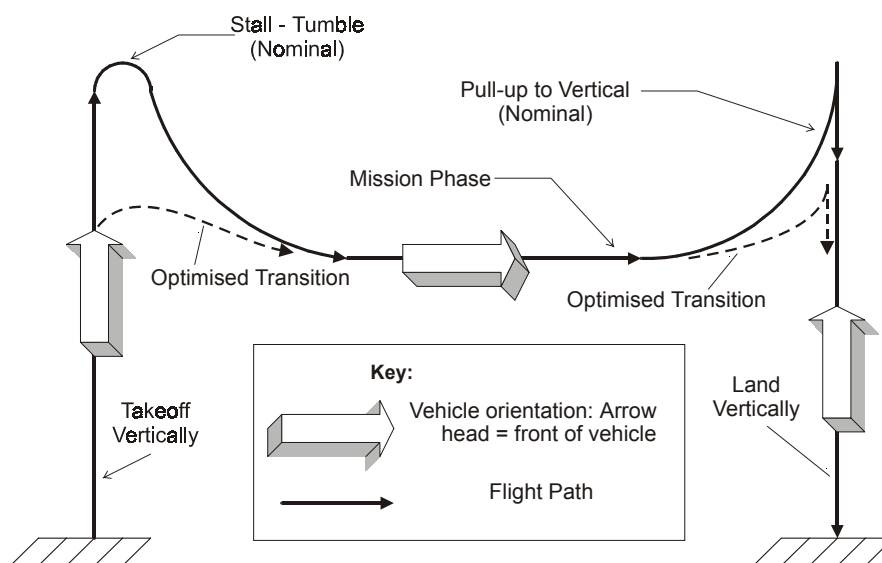


Figure 5: T-Wing Vehicle Flight Path

Reasons for Optimisation of Transition Manoeuvres

The transition manoeuvres described in the previous section will affect the operational utility of the vehicle in a number of ways. Some of these are listed below.

- The transitions should take as little time to complete as possible to enable the vehicle to quickly enter and exit the mission phase of its flight regime.
- The vehicle should gain as little excess height as possible during these manoeuvres to minimise possible conflict with overlying airspace and in the military case to minimise the chance of being detected.
- The vehicle should if possible avoid excessive angle of attack regions where the simulation and analysis is uncertain.
- A last reason to also avoid stalled flight conditions or “tumble” manoeuvres is because they worry potential users.

With these considerations in mind some work has been done in performing numerical optimisations of the transition manoeuvres to try and achieve the above goals. So far this work has only looked at the take-off, (vertical to horizontal transition) manoeuvre; the landing manoeuvre will be looked at in the future. Before describing the current work it is necessary to give some background as regards the 6 DOF simulation model of the vehicle as this was used for all the manoeuvre optimisation work.

6 DOF Non-Linear Simulation of Vehicle

The starting point for the work done on transition manoeuvre optimisation is a full non-linear 6-DOF[‡] model of the T-Wing vehicle that has been developed by the author at the University of Sydney over the past 3 years². Basically this model consists of the normal non-linear 6-DOF equations of motion that apply to any vehicle, a simple mass model of the vehicle and a large database of basic forces (or coefficients) and aerodynamic derivatives covering a large number of flight conditions. In the current model the following ranges of speed, angles of attack and sideslip, and thrust settings are covered.

$$V = [1,10,30,70,100,140,190] \text{ ft/sec}$$

$$\alpha = \pm[0,9,12,15,18,24,30,50,70,90]^\circ$$

$$\beta = [0,10,30,50,70,90]^\circ$$

$$\delta_{throttle} = [0.4,0.7,1.0]$$

It should be noted that the extreme angles of attack and sideslip ($>30^\circ$) are not run for velocities above 70 ft/sec. This thus gives a total of in excess of 2000 flight conditions in the database. Intermediate conditions are found via simple interpolation. While it may seem unusual to make provisions for such large angles of attack and sideslip in an air-vehicle simulation this is necessary for the T-Wing vehicle as, for instance, it will be required to hover in crosswinds leading to an angle of attack of 90° . To obtain realistic aerodynamic forces and coefficients at these large angles has been one of the most challenging aspects of preparing the T-Wing simulation model.

Aerodynamic and Propulsion Model

A fixed wake panel method model is used to capture the aerodynamic characteristics of the vehicle³. This is coupled with a blade element solution for the propellers to allow the prediction of the slipstream characteristics, which are critical in hover flight, where vehicle control is effected via prop-wash over wing and fin mounted control surfaces. The blade-element solution also gives the propeller forces for any flight condition. Both the blade

[‡] Because the transition maneuvers considered here all occur in the body axis xz plane, only 3 of the 6 DOF were actually exercised during the optimization of these maneuvers.

element and the panel method calculations use judicious 2D viscous corrections to achieve more realistic results in the presence of non-linear effects such as wing, canard and blade stall. It should also be realized that although the aerodynamic database goes into extreme angle of attack regions of the flight envelope it mainly does so at relatively low speeds where the forces on the vehicle are dominated by the forces in the (un-stalled) slipstream. Thus in many respects the high α and β regions on the vehicle act as second order corrections to the loads generated at more reasonable flow angles in the slipstream.

A typical aerodynamic model of a T-Wing vehicle is shown in Figure 6 indicating the pressure field over the vehicle for a cruise flight condition.

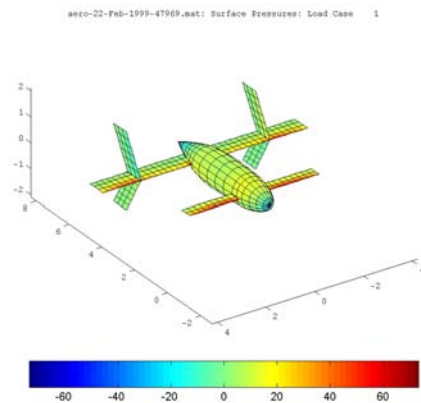


Figure 6: Aerodynamic Model of Vehicle, (Dimensions in ft; Pressure in psf)

Real Time Flight Simulation

The actual simulation model is currently implemented in the SIMULINK⁴ environment and has now been refined to run in real time via use of an add-on product, The Real Time Workshop⁵. This is a significant advance on the previous simulation work, which ran at approximately 1/30th of actual speed.

One of the primary results of this is the development of a visual pilot training simulator, which allows a ground based remote pilot to practice *manual* flight of the vehicle without risking an airframe. This is required because the technology demonstrator vehicle is initially being test flown without any automatic controls in place. The real-time simulation is also currently being used to develop stability augmentation systems for the vehicle and will also be used in the development of full autonomous controllers for the vehicle.

However, for the purposes of this paper, the importance of the faster simulation is that it has made the numerical optimization of the transition maneuvers tractable. This is because a 10 second simulation can be run in about 0.3 seconds and hence the large number of function evaluations required by numerical optimizers can now be accommodated in a reasonable time.

A figure showing snap-shots of a typical vehicle undergoing a vertical to horizontal transition maneuver under rudimentary automatic control is given in Figure 7.

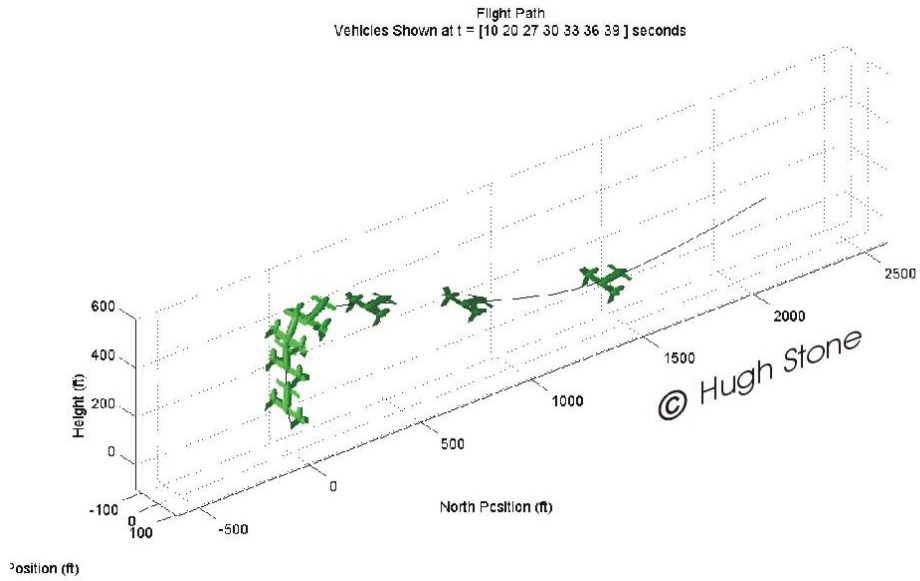


Figure 7: Typical Simulation of Vertical to Horizontal Transition Under Automatic Control: (unequal time increments).

Optimisation of Transition Manoeuvres

Statement of Problem

The basic idea in the work done on optimizing the take-off transition manoeuvre has been to get the vehicle from zero speed on the ground, to a specified altitude at a specified speed in the minimum amount of time. It was also specified that at this point, (when the vehicle was considered to be flying), it should not be descending; that during the transition it should not impact the ground; and that its angle of attack should remain within reasonable bounds. In mathematical terms the optimization problem was framed in the following way.

$$f = t_{exit} \quad (1)$$

$$g_1 = 100ft - h_{exit} \quad (2)$$

$$g_2 = -\gamma_{exit} \quad (3)$$

$$g_3 = |\alpha| - 12 \quad (4)$$

$$g_4 = -h \quad (5)$$

where :

- t_{exit} = the time to reach a velocity of 100 ft/sec
- f = cost function (to be minimised)
- h_{exit} = vehicle height above ground at t_{exit}
- γ_{exit} = vehicle flight path angle at t_{exit}
- α = vehicle angle of attack, (at any point of maneuver)
- h = vehicle height above ground, (at any point of maneuver)
- g_i = constraint functions; less than zero to be satisfied, ($i = 1, \dots, 4$)

The inputs to the simulation function were simply a series of elevator deflection angles at a number of different instants of time. These were coded in an optimisation vector variable in the following way.

$$x = [\delta_{el_1}, \Delta t_1, \delta_{el_2}, \Delta t_2, \dots, \delta_{el_n}, \Delta t_n] \quad (6)$$

where :

- δ_{el_i} = the i'th elevator deflection angle
- Δt_i = the duration of this deflection

Typically “n” was set to 6 or 7, which meant that the average length of each input was between 1 and 2 seconds, (Most transitions took place within 7 to 12 seconds, depending on the MTOW of the vehicle).

To start an optimisation run, a mass for the vehicle was specified along with an initial guess for “x”, the vector of elevator deflections and deflection times. These were then passed to the numerical optimisation routine, (an SQP routine implemented in MATLAB⁶) which at each stage ran the simulation as it altered the “x” vector to try and achieve the minimum time to complete the transition while not violating any of the constraints. For all transitions the throttle was assumed to be fully open, ($\delta_{throttle} = 1.0$).

Results

Optimisations were run for a constant vehicle configuration, though the mass of the vehicle was varied between runs to see the effect of this on the optimal transition manoeuvre. The masses for which optimisations were run are given in Table 1, and are also shown in Figure 8.

Mass (slugs)	Mass (lb _m)	Transition Time (s)	Notes
1.60	51.5	5.18	
1.80	58.0	6.29	
1.90	61.2	7.00	
2.00	64.4	7.91	
2.10	67.6	9.43	
2.15	69.2	10.27	
2.20	70.8	11.53	Didn't quite converge

Table 1: Masses for Maneuver Optimisation Runs

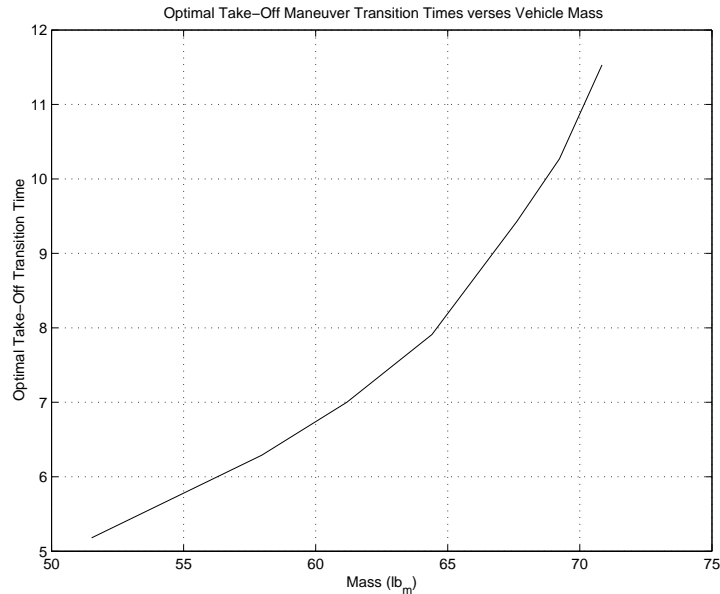


Figure 8: Optimal Transition Times vs Vehicle Mass

Besides looking at the time to perform the transitions in comparison to the vehicle mass it is also worthwhile looking at the differences between transition maneuvers for different mass vehicles. Graphs of the actual transition flight paths for vehicle masses of 1.60 slugs (51.5 lb) and 2.15 slugs (69.2 lb) are given in Figure 9 and Figure 10. Graphs of the angle of attack (α), pitch attitude (θ) and flight path angle (γ) for these same masses are given in Figure 11 and Figure 12. Graphs showing the optimized elevator command history for these cases are given in Figure 13 and Figure 14. From these graphs the following comments can be made regarding the transition maneuvers and their sensitivity to vehicle mass.

- It does not appear in any of the vehicles investigated thus far (ranging between 51.5 and 69.2 lb in weight) that a large altitude loss is present in the optimal take-off transition maneuvers. In fact, for the lighter weights it is clear that the vehicle is simply able to “climb” directly into forward flight. As the hover thrust for all the vehicles is constant (~80 lbf), the lighter vehicles have significantly greater thrust to weight ratios than the heavier ones: the results here correspond to vehicles with ratios between 1.55 and 1.16. It is clear however that the “optimal” maneuvers tend toward exhibiting a more pronounced altitude loss as mass is increased. For masses above the range shown it is expected that a more pronounced altitude loss will be experienced in performing the transition maneuver. This is suggested by results at a mass of 2.20 slugs (70.8 lb) where convergence problems were found in the optimization. By looking at the “not-quite-converged” flight path for this mass (Figure 15) it is clear that more of an altitude loss is present.
- The graphs also show that as the mass is increased (excess thrust decreased) the optimal takeoff transition maneuvers exhibit increased angles of attack for greater portions of the maneuver. This is clear by comparing the angles of attack for the 1.60 slug vehicle, where the angle of attack throughout the maneuver remains close to zero, (Figure 11) and the 2.15 slug case where it stays close to the constraint value of 12° for much of the transition (Figure 12). The not-quite-converged results for a mass of 2.20 slugs (Figure 16) amplify this observation.
- Because the optimal transition maneuvers were always constrained to stay out of stalled regions it can be seen that it is quite possible to perform the transition without any actual stalled flight. At heavier vehicle weights it may not however be possible to perform the maneuver without loss of altitude. For this reason the name “stall-tumble” is perhaps misleading.

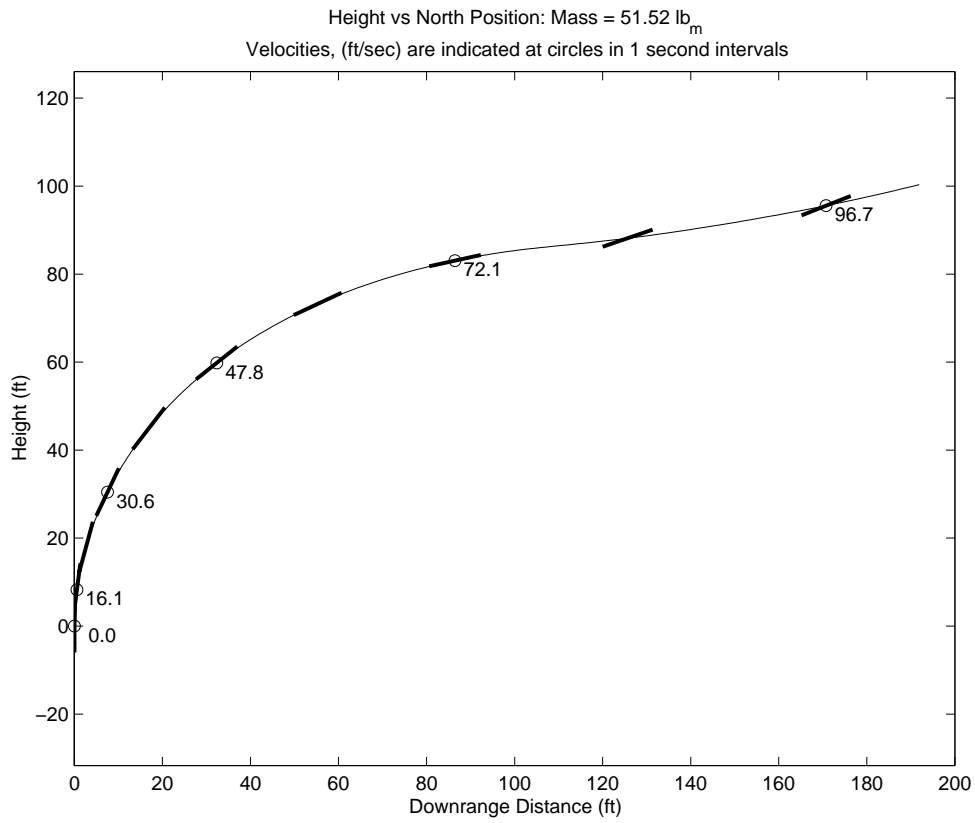


Figure 9: Transition Flight Path: (Mass = 1.60 slugs)

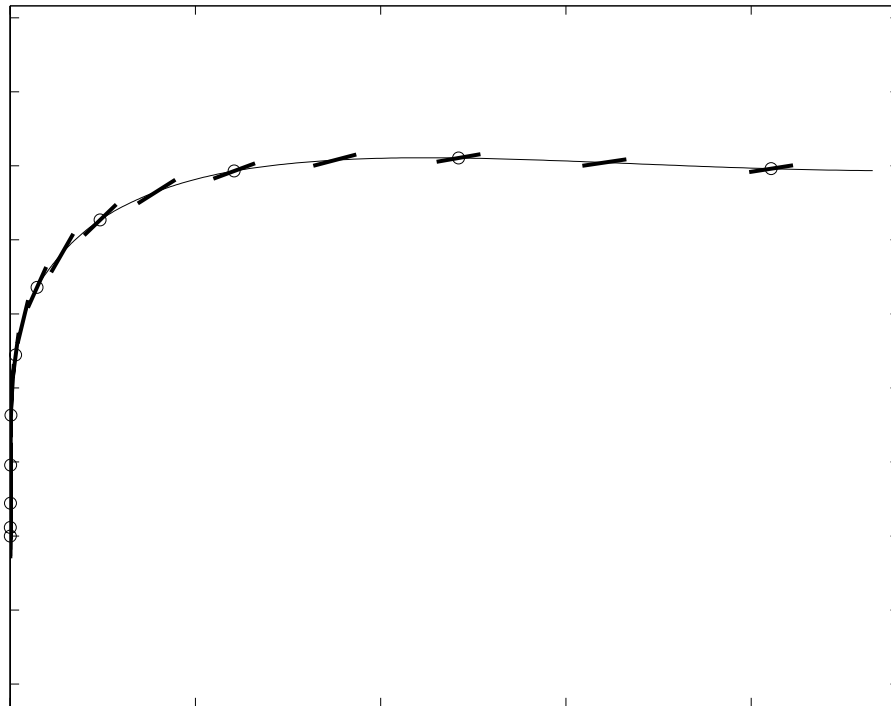


Figure 10: Transition Flight Path, (Mass = 2.15 slugs)

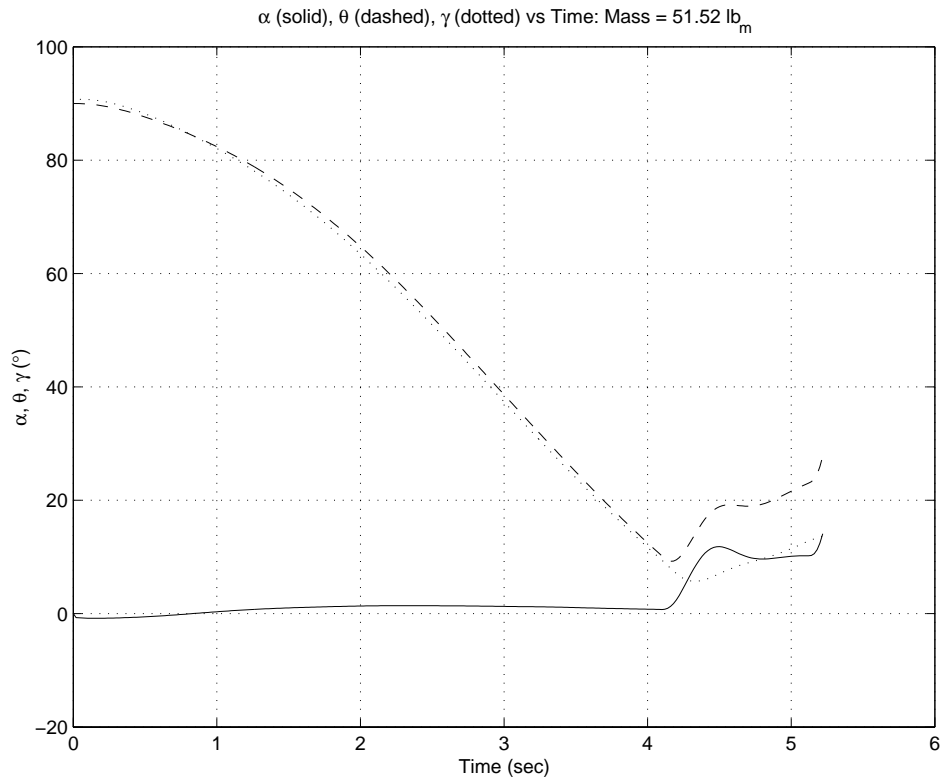


Figure 11: Angle of Attack (α), Pitch Attitude (θ) and Flight Path Angle (γ) vs Time, (Mass = 1.60 slugs)

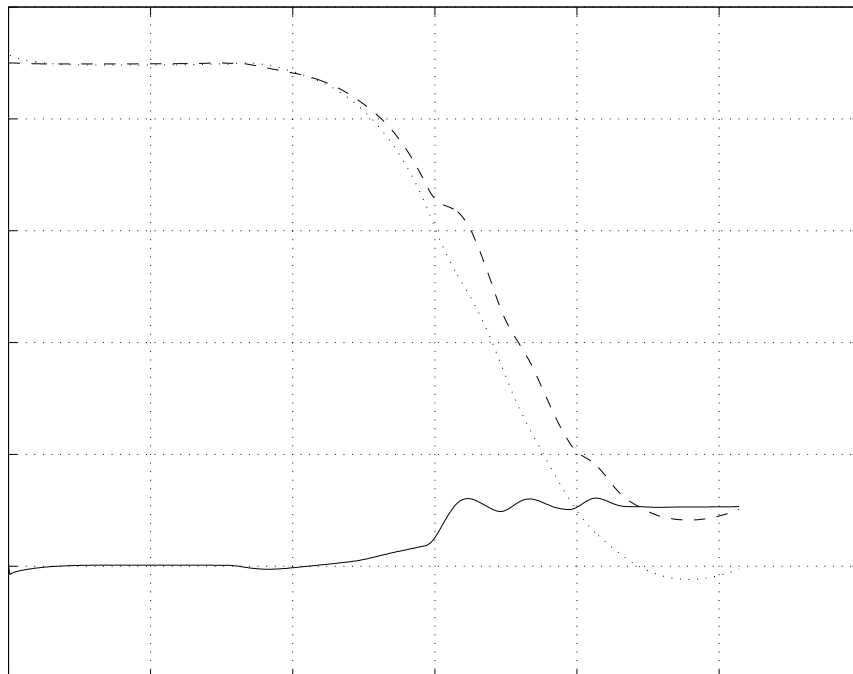


Figure 12: Angle of Attack (α), Pitch Attitude (θ) and Flight Path Angle (γ) vs Time, (Mass = 2.15 slugs)

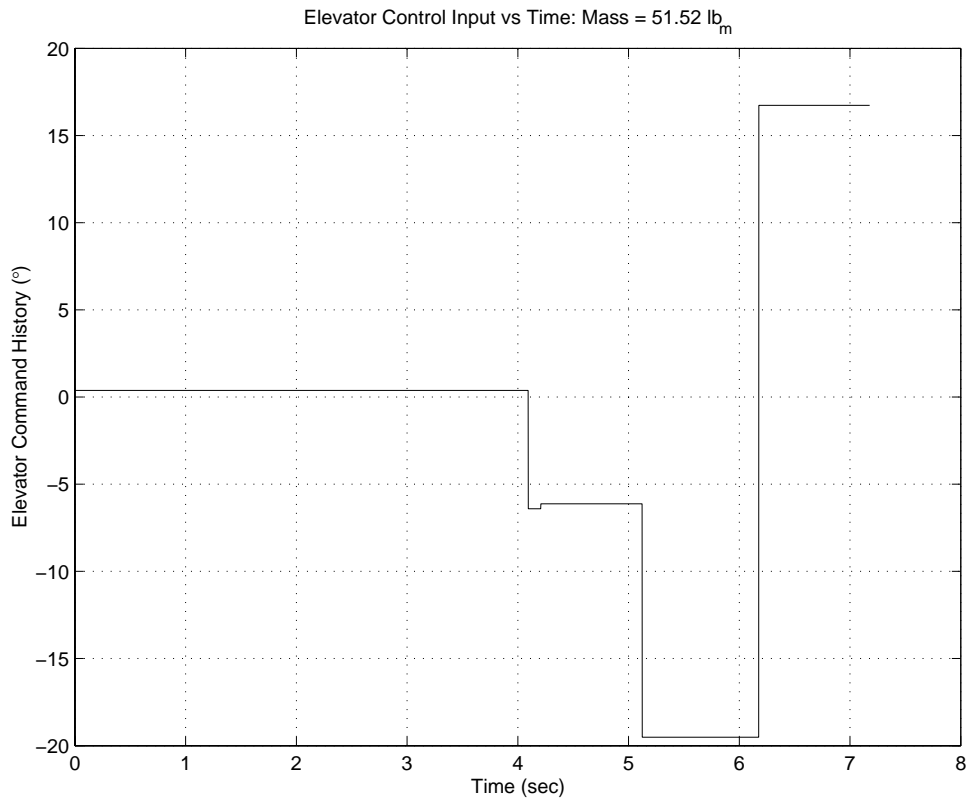


Figure 13: Elevator Command History As Optimised, (Mass = 1.60 slugs)

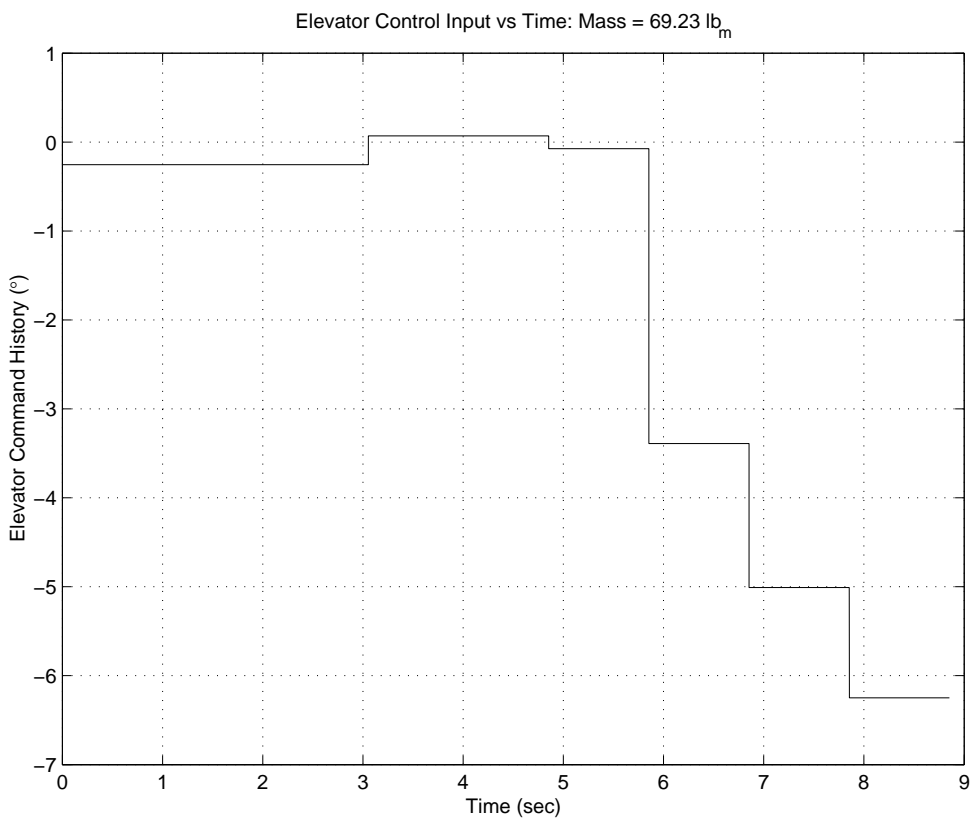


Figure 14: Elevator Command History As Optimised, (Mass = 2.15 slugs)

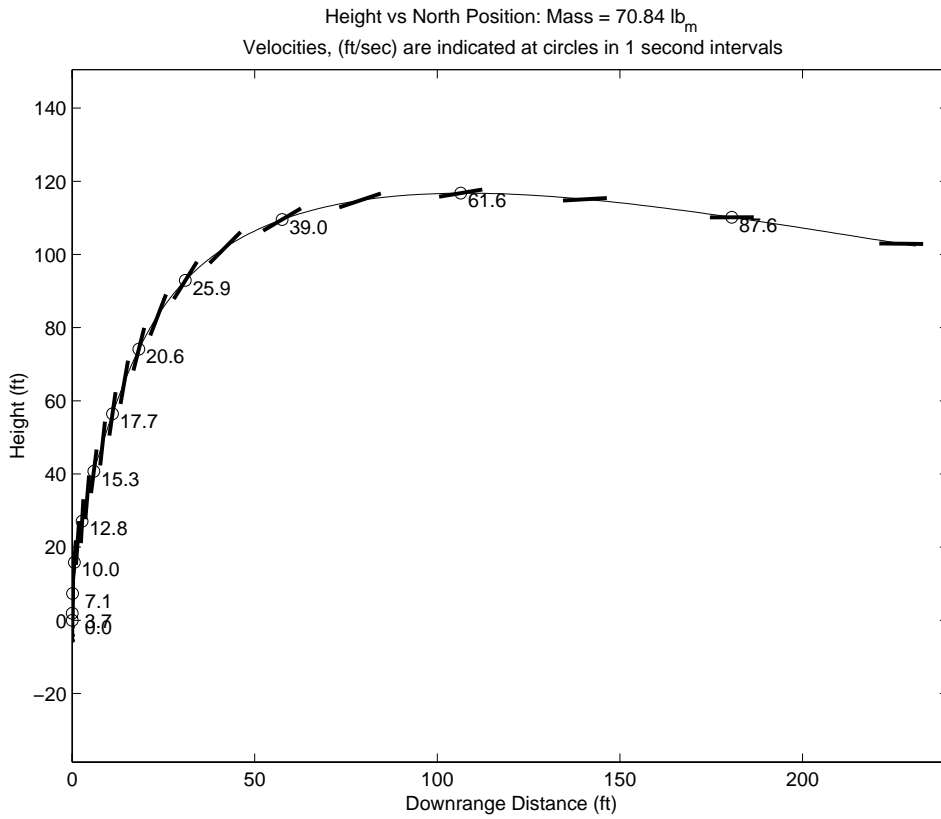


Figure 15: Transition Flight Path (Not quite converged: Mass = 2.20 slugs)

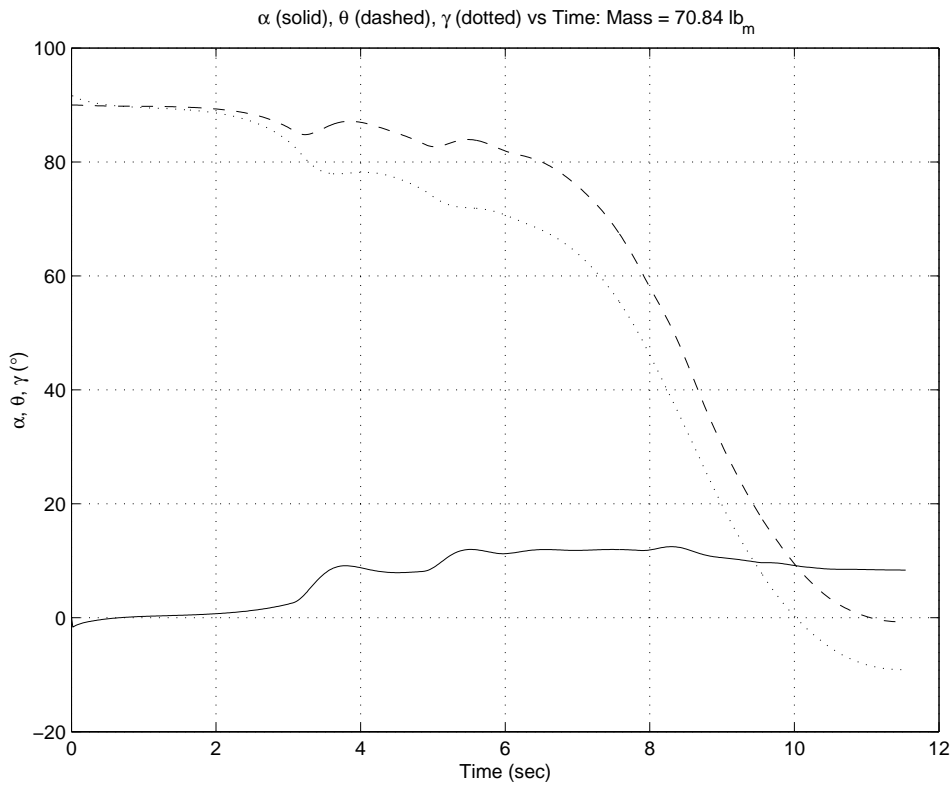


Figure 16: (Angle of Attack (α), Pitch Attitude (θ) and Flight Path Angle (γ) vs Time (Not quite converged: Mass = 2.20 slugs)

Conclusion

In conclusion it can be seen that it is in fact possible to perform the take-off transition manoeuvre for the T-Wing vehicle without significant altitude loss at the top of the manoeuvre for static thrust to weight ratios down to as low as 1.15. Below this level it is to be expected that an un-stalled transition will have to be accompanied by a more significant altitude loss. It should be pointed out that these results are specific to the T-Wing vehicle and cannot necessarily be extrapolated to other tail-sitter vehicles with a high degree of precision. For instance, different propellers will have different thrust-loss characteristics as the forward speed of the vehicle is increased and this could change the results significantly. Lastly it can be seen that a relatively straightforward numerical optimisation analysis based on a good non-linear vehicle simulation can provide useful information for improving the operational effectiveness of the T-Wing vehicle. Similar techniques will also be applied in the future to the reverse transition manoeuvre.

References

-
- ¹ C. Hutchison. *The Airframe and Producibility Redesign of the "T-Wing" Unmanned Aerial Vehicle*, Undergraduate Thesis, University of Sydney, NSW, Australia, November 2000.
 - ² R.H. Stone. *Configuration Design of a Canard Configured Tail-Sitter Unmanned Vehicle Using Multidisciplinary Optimisation*, PhD Thesis, University of Sydney, Sydney, Australia, 1999.
 - ³ J. Katz and A. Plotkin. *Low-Speed Aerodynamics: From Wing Theory to Panel-Methods*. McGraw-Hill Book Company, New York, 1991.
 - ⁴ *SIMULINK Manual*. The Math Works Inc, 2000.
 - ⁵ *Real Time Workshop Manual*, The Math Works Inc, 2000.
 - ⁶ *MATLAB Manual*, The Math Works Inc, 2000.